PERFORMANCE ENHANCING OF 3-PHASE UPQC USING FEEDBACK LINEARISATION BASED DPC TECHNIQUE FOR POWER QUALITY IMPROVEMENT

Dahdouh Adel[a,*], Mazouz Lakhdar[b], Brahim Elkhalil Youcefa [c]

[a,b,c] Applied Automation and Industrial Diagnostic Laboratory, Electrical Engineering Department.
Faculty of Science and Technology, Djelfa University, 17000 Djelfa, Algeria

Adel.dahdouh@univ-djelfa.dz, l.mazouz@univ-djelfa.dz, khalilyoucefa@gmail.com

Abstract

This paper presents the compensation principle using feedback linearization based DPC control strategies of the unified power quality conditioner, which aims at the integration of series-active and shunt-active power filters. In order to improve the performances of UPQC, a control method based on a feedback linearization based DPC controller combined with space vector modulation (SVM) is proposed. The purposes are to deliver compensation signals more quickly and accurately at varied load conditions and to eliminate voltage as well as current harmonics with good dynamic response. Extensive simulation results obtained by Matlab/Simulink for a passive load connected through an uncontrolled bridge rectifier validate the performance of the suggested control scheme. The comparison of these results with those obtained with a PI controller demonstrates the superiority of the proposed controller.

Keywords

Harmonic extraction, Power active filter, UPQC, Feedback linearization controller, DPC, Space vector modulation (SVM).

1. INTRODUCTION

In recent years, the increasing use of power electronic devices has led to the deterioration of power quality due to harmonic generations [1]. The terminology and the guidelines for power quality have been described in detail at IEEE-519 and IEC-555. According to these guidelines, the allowed total harmonic distortion should be less than 5% [2].

The aforementioned problems are partially solved with the help of passive filters [3-5]. However, this kind of filter cannot solve random variations in the load current waveform and voltage waveform. On the other hand, compensating devices such as Static Var Compensator (SVC), Parallel Active Filter (PAF), Series Active Filter (SAF), and hybrid filters are proposed to ensure power quality [6]. However, their capabilities are usually limited as they can only solve one or two power quality problems. Recent research has shown that the unified power quality conditioners (UPQCs), an integration of series and shunt active filters, can be utilized to solve most power quality problems simultaneously [7].

The UPQC can maintain the load end-voltage at the desired level and prevent incoming sags/swells in voltages [8]. In addition the UPQC can efficiently support the reactive power requirement of the load, and suppress the generated load harmonic currents, so that do not propagate back to the utility, which can cause voltage and current distortion to other consumers [9].

Different control approaches for the UPQC have been pro-posed. In [11] authors have applied a linear control using PI controller. The control of the UPQC connected to a Wind system by PI controller is proposed in [12]. An intelligent controller has been applied by [13] and [14]. A four wire topology of the UPQC controlled by PI has been studied in [15], [16] and [17].

The aim of this paper is twofold. Firstly, to design a feedback linearization based DPC controller combined with space vector modulation for the UPQC to enhance power quality. secondly, to compare the performances of the proposed controller with a PI controller to validate the proposed controller, through an extensive simulation results for a passive load connected through an uncontrolled bridge rectifier.

The rest of the paper is organized as follows: in section II, the control design of the UPQC is presented, while in section III, simulation results and their discussion are given, finally a conclusion of the present work is derived.

2. CONTROL DESIGN

2.1 Mathematical Model of UPQC

The differential equations describing the dynamic model of UPQC are defined in stationary α-β reference frame, as given in equations (1) and (2).

The parallel filter model is governed by the following equation.

$$\dot{x}_p = f_p(x_p) + g_p(x_p)u_p \tag{1}$$

where:

$$f_p(x_p) = \begin{bmatrix} -\frac{R_{fp}}{L_{fp}}x_{p1} \\ -\frac{R_{fp}}{L_{fp}}x_{p2} \end{bmatrix}, g_p(x_p) = \begin{bmatrix} \frac{1}{L_{fp}} & 0 \\ 0 & \frac{1}{L_{fp}} \end{bmatrix}, x_p = \begin{bmatrix} P_{fp} \\ Q_{fp} \end{bmatrix}, u_p = \begin{bmatrix} V_{fp\alpha} \\ V_{fp\beta} \end{bmatrix}$$

$$y_p = \begin{bmatrix} y_{p1} \\ y_{p2} \end{bmatrix} = \begin{bmatrix} h_{p1} \\ h_{p2} \end{bmatrix}$$

$V_{fp\alpha\beta}$, P_{fp} and Q_{fp} are the voltages and active and reactive powers of the shunt filter respectively.

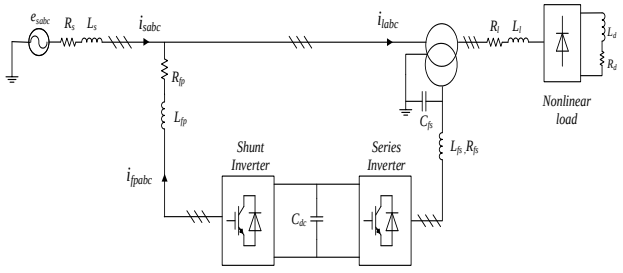

Figure. 1. Single-line scheme of the UPQC .

The series filter model is described by:

$$\dot{x}_s = f_s(x_s) + g_s(x_s)u_s \tag{2}$$

Where: $f_s(x_s) = \begin{bmatrix} \frac{1}{C_{fs}} x_{s1} \\ \frac{1}{C_{fs}} x_{s2} \end{bmatrix}$, $g_s(x_s) = \begin{bmatrix} \frac{1}{L_{fs}} & 0 \\ 0 & \frac{1}{L_{fs}} \end{bmatrix}$, $x_s = \begin{bmatrix} P_{fs} \\ Q_{fs} \end{bmatrix}$, $u_s = \begin{bmatrix} V_{fs\alpha} \\ V_{fs\beta} \end{bmatrix}$

$$y_s = \begin{bmatrix} y_{s1} \\ y_{s2} \end{bmatrix} = \begin{bmatrix} h_{s1} \\ h_{s2} \end{bmatrix}$$

$V_{fs\alpha\beta}$, P_{fs} and Q_{fs} are the voltages and active and reactive powers of the series filter respectively.

2.2 Harmonic extraction

Active filter depends greatly on the extraction method used to eliminate harmonics from the distorted waveforms [18], [19]. Hereafter, harmonics extraction methods are described.

2.2.1 Harmonic currents extraction using PQ theory

In this work the instantaneous power theory technique (PQ theory) is chosen as highlighted in Fig. 2.

Instantaneous active and reactive powers of the nonlinear load are calculated by:

$$\begin{bmatrix} P_l \\ Q_l \end{bmatrix} = \begin{bmatrix} v_{s\alpha} & v_{s\beta} \\ v_{s\beta} & -v_{s\alpha} \end{bmatrix} \begin{bmatrix} i_{l\alpha} \\ i_{l\beta} \end{bmatrix} \tag{3}$$

Where the instantaneous powers can be expressed as follows:

$$\begin{cases} P_l = \bar{P}_l + \tilde{P}_l \\ Q_l = \bar{Q}_l + \tilde{Q}_l \end{cases} \tag{4}$$

For harmonic and reactive power compensation, all of the reactive power ($\bar{Q}_l$ and $\tilde{Q}_l$ components) and harmonic component ($\tilde{P}_l$) of active power are selected as compensation power references and the compensation currents reference are calculated as (5).

$$\begin{bmatrix} i^*_{fp\alpha} \\ i^*_{fp\beta} \end{bmatrix} = \frac{1}{v^2_{s\alpha} + v^2_{s\beta}} \begin{bmatrix} v_{s\alpha} & v_{s\beta} \\ v_{s\beta} & -v_{s\alpha} \end{bmatrix} \begin{bmatrix} \tilde{P}_l \\ Q_l \end{bmatrix} \tag{5}$$

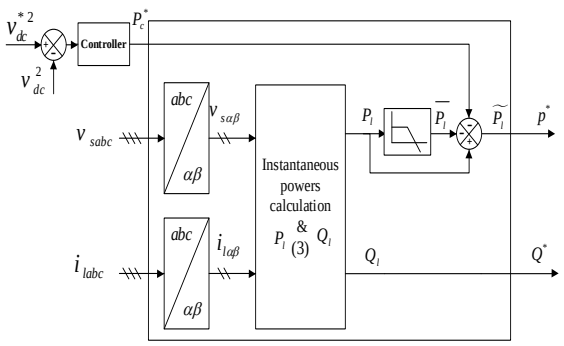

Figure. 2. Harmonic currents extraction scheme using PQ theory

On the other hand the signal P_c^* is used as an average real power, and is obtained from the DC voltage controller.

2.2.3 Harmonic voltages extraction using PQ-PLL theory

It consists of two parts, the first is to extract voltage harmonics, and it is similar to PQ theory for currents (Equation (6)).

$$\begin{bmatrix} \overline{v_{s\alpha}} \\ \overline{v_{s\beta}} \end{bmatrix} = \frac{1}{i^2_{l\alpha} + i^2_{l\beta}} \begin{bmatrix} i_{l\alpha} & i_{l\beta} \\ -i_{l\beta} & i_{l\alpha} \end{bmatrix} \begin{bmatrix} \overline{P_l} \\ \overline{Q_l} \end{bmatrix} \tag{6}$$

The second part is to calculate the voltage drop across the load as shown in Fig. 3.

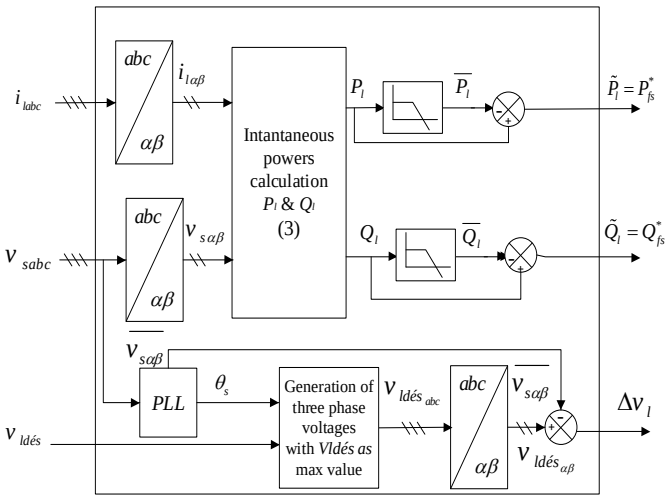

Figure. 3. Harmonic voltages extraction scheme using PQ-PLL theory .

2.3 Feedback Linearisation Controller (FLC) Synthesis

Consider the nonlinear system represented by:

$$\dot{x} = f(x) + \sum_{i=1}^{p} g_i(x)u_i \qquad i = 1, 2, ..., p$$
$$y_i = h_i(x) \tag{7}$$

where g(x) and f(x) are scalar functions.

The well-known method to form feedback linearization law of the previous system is shown in Fig. 4 [20]. The problem of finding the vector relative degree of the system (7) implies differentiation of each output signal until one of the input signals appear explicitly in the differentiation. For each output signal, we define r_j as the smallest integer such that at least one of the inputs appears in $y_j^{(r_j)}$ [9]:

$$y_j^{(r_j)} = L_f{}^{r_j} h(x) + \sum_{i=1}^{p} L_{gi}(L_f{}^{r_j - 1} h_j(x))u_i \quad j = 1, 2, ..., p \tag{8}$$

Where: $L_f h_j$ and $L_{gi}(L_f{}^{r_j - 1} h_j)$ stand for *Lie derivatives* of *h* with respect to *f* and *g*, respectively.

The global relative degree (*r*) is defined as the sum of all the relative degrees obtained using (8). It must be less than or equal to the order of the system: $r = \sum_{j=1}^{p} r_j \le n$

To find the expression of linearizing law *u* that allows making linear the relationship between inputs and outputs, the expression (8) can be written in its matrix form:

$$[y_1^{r_j} \ \ldots \ \ldots y_p^{r_p}]^t = \zeta(x) + D(x)u \tag{9}$$

Where:

$$\zeta(x) = \begin{pmatrix} L_f{}^{r_1} h_1(x) \\ L_f{}^{r_2} h_2(x) \\ \cdot \\ \cdot \\ \cdot \\ L_f{}^{r_p} h_p(x) \end{pmatrix} \tag{10}$$

And

$$D(x) = \begin{pmatrix} L_{g_1} L_f{}^{r_1-1} h_1 & L_{g_2} L_f{}^{r_1-1} h_1 & \ldots & L_{g_p} L_f{}^{r_1-1} h_1 \\ L_{g_1} L_f{}^{r_2-1} h_2 & L_{g_2} L_f{}^{r_2-1} h_2 & \ldots & L_{g_p} L_f{}^{r_2-1} h_2 \\ \cdot & \cdot & \ldots & \cdot \\ L_{g_1} L_f{}^{r_p-1} h_p & L_{g_2} L_f{}^{r_p-1} h_p & \ldots & L_{g_p} L_f{}^{r_p-1} h_p \end{pmatrix} \tag{11}$$

$D(x)$ is called the decoupling matrix system.
Assuming that D(x) is not singular, the linearizing control law has the following form [9]:

$$u = D(x)^{-1}(-\zeta(x) + v) \tag{12}$$

Notice that linearization would be possible only if the decoupling matrix D(x) is reversible. The block diagram of the linearized system is given in figure (4).

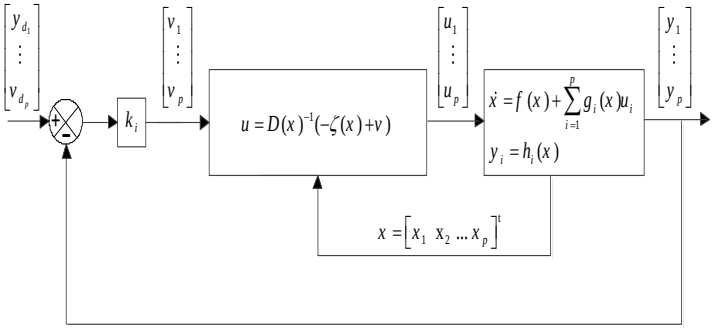

Figure. 4. Block diagram of linearized MIMO system.

2.3.1 DC voltage FLC synthesis

The synthesis of the DC voltage controller is based on the second subsystem. The derivative of the output $y=h = v_{dc}{}^2$ is given by:

$$\dot{y} = L_f h(x) + L_g h(x)u = \frac{2}{C_{dc}} P_{dc} \tag{13}$$

The control input P_{dc} appear in (15), so the relative degree is r =1. The relative degree of this output is equal to the order of subsystem 2, which corresponds clearly to an exact linearization [10].

Then the control law is obtained by:

$$P_{dc}^* = 2C_{dc}v \tag{14}$$

where: $\dot{y} = v$

For a problem of trajectory tracking defined by v_{dc}*(t), the term v is expressed by:

$$v = k_{dc}(v_{dc}^{*2} - v_{dc}^2) + \frac{dv_{dc}^{*2}}{dt} \tag{15}$$

Where, k_{dc} is a positive constant

2.3.2 Parallel powers FLC synthesis

Each output derivative is given by:

$$\dot{y}_j = L_f\ h(x) + \sum_{i=1}^{2} L_{gi}(L_f\ h_j(x))u_i \quad j = 1,2 \tag{16}$$

Then (16) can be written in matrix form as:

$$\begin{bmatrix} \dot{y}_1 \\ \dot{y}_2 \end{bmatrix} = \begin{bmatrix} -\frac{R_{fp}}{L_{fp}} x_{p1} \\ -\frac{R_{fp}}{L_{fp}} x_{p2} \end{bmatrix} + \begin{bmatrix} \frac{1}{L_{fp}} & 0 \\ 0 & \frac{1}{L_{fp}} \end{bmatrix} \begin{bmatrix} u_1 \\ u_2 \end{bmatrix} \tag{17}$$

The decoupling matrix determinant is different to zero, and then the control law is given as:

$$u = \begin{bmatrix} u_1 \\ u_2 \end{bmatrix} = D(x)^{-1}\left[-\zeta(x) + \begin{bmatrix} v_1 \\ v_2 \end{bmatrix}\right] \tag{18}$$

The application of the linearization law on the first subsystem leads to the following decoupled linear system:

$$\begin{bmatrix} \dot{y}_1 \\ \dot{y}_2 \end{bmatrix} = \begin{bmatrix} v_1 \\ v_2 \end{bmatrix} \tag{19}$$

The control law used for tracking is:

$$\begin{aligned} v_1 &= k_{p1}(P_{fp}^* - P_{fp}) + \frac{dP_{fp}^*}{dt} \\ v_2 &= k_{p2}(Q_{fp}^* - Q_{fp}) + \frac{dQ_{fp}^*}{dt} \end{aligned} \tag{20}$$

Where k_{p1} and k_{p2} are positive constants.

2.3.3 Series powers FLC synthesis

Each output derivative is given by:

$$\dot{y}_j = L_f\ h(x) + \sum_{i=1}^{2} L_{gi}(L_f\ h_j(x))u_i \quad j = 1,2 \tag{21}$$

Then (21) can be written in matrix form as:

$$\begin{bmatrix} \dot{y}_1 \\ \dot{y}_2 \end{bmatrix} = \begin{bmatrix} -\frac{R_{fs}}{L_{fs}} x_{s1} \\ -\frac{R_{fs}}{L_{fs}} x_{s2} \end{bmatrix} + \begin{bmatrix} \frac{1}{L_{fs}} & 0 \\ 0 & \frac{1}{L_{fs}} \end{bmatrix} \begin{bmatrix} u_1 \\ u_2 \end{bmatrix} \tag{22}$$

The decoupling matrix determinant is different to zero, and then the control law is given as:

$$u=\begin{bmatrix}u_1\\u_2\end{bmatrix}=D(x)^{-1}\left[-\zeta(x)+\begin{bmatrix}v_1\\v_2\end{bmatrix}\right] \tag{23}$$

The application of the linearization law on the first subsystem leads to the following decoupled linear system:

$$\begin{bmatrix}\dot{y}_1\\\dot{y}_2\end{bmatrix}=\begin{bmatrix}v_1\\v_2\end{bmatrix} \tag{24}$$

The control law used for tracking is:

$$\begin{aligned}v_1&=k_{s1}(P_{fs}^{*}-P_{fs})+\frac{dP_{fs}^{*}}{dt}\\v_2&=k_{s2}(Q_{fs}^{*}-Q_{fs})+\frac{dQ_{fs}^{*}}{dt}\end{aligned} \tag{25}$$

Where k_{s1} and k_{s2} are positive constants.

2.4 Space Vector Modulation

In this section, SVM technique is presented to produce PWM control signals (s_a, s_b and s_c) to the power switches of the inverter. SVM compensates the required volt-seconds using discrete switching states and their on-times. The space vector diagram of a three phase voltage source inverter is a hexagon (Fig. 5), consisting of six sectors. Every sector is an equilateral triangle of a height h =√3/2 [23]. For any given reference vector, the sector of operation is determined by using Eq (26).

$$S_i=\text{int}(\frac{\theta_s}{60})+1 \tag{26}$$

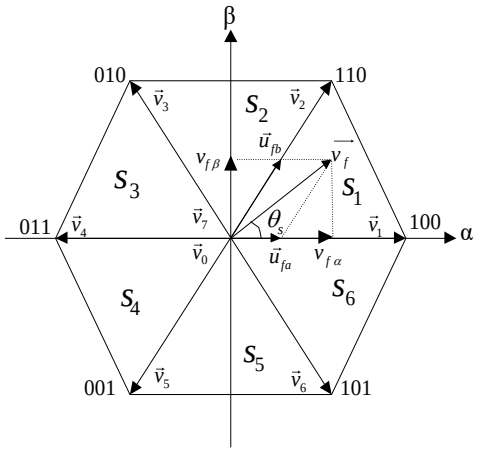

Figure. 5. Space vector diagram.

The on-time calculation is similar for all sectors. Volt-second equation is given by:

$$\vec{v_f}T_s=t_i\vec{v_i}+t_{i+1}\vec{v}_{i+1}+t_0\vec{v}_0 \tag{27}$$

where $T_s = 1/f_s$, with f_s is the switching frequency.
In the first sector,

$$\begin{cases}\vec{v}_1=\sqrt{\frac{2}{3}}v_{dc}\\\vec{v}_2=\sqrt{\frac{2}{3}}v_{dc}(\frac{1}{2}+j\,\frac{\sqrt{3}}{2})\\\vec{v}_0=0\end{cases} \tag{28}$$

The reference vector can be also written as follows,

$$\vec{v_f}=v_{f\alpha}+jv_{f\beta} \tag{29}$$

From Equations (27, 28 and 29) one can find:

$$\begin{cases}v_{f\alpha}=\sqrt{\frac{2}{3}}v_{dc}\frac{t_1}{T_s}+\frac{1}{\sqrt{6}}v_{dc}\frac{t_2}{T_s}\\v_{f\beta}=\frac{1}{\sqrt{2}}v_{dc}\frac{t_2}{T_s}\end{cases} \tag{30}$$

From equation (30), ON times calculation are given below

$$\begin{cases}t_1=\frac{\sqrt{6}v_{f\alpha}-\sqrt{2}v_{f\beta}}{v_{dc}}T_s\\t_2=\frac{\sqrt{2}v_{f\beta}}{v_{dc}}T_s\\t_0=T_s-(t_1+t_2)\end{cases} \tag{31}$$

The choice of the null vector determines the SVM scheme. There are a few options: the null vector v_0 only, the null vector v_7 only, or a combination of the null vectors. A popular SVM technique is to alternate the null vector in each cycle and to reverse the sequence after each null vector as shown in Fig. 6. This will be referred to as the symmetric 7-segment technique [24].

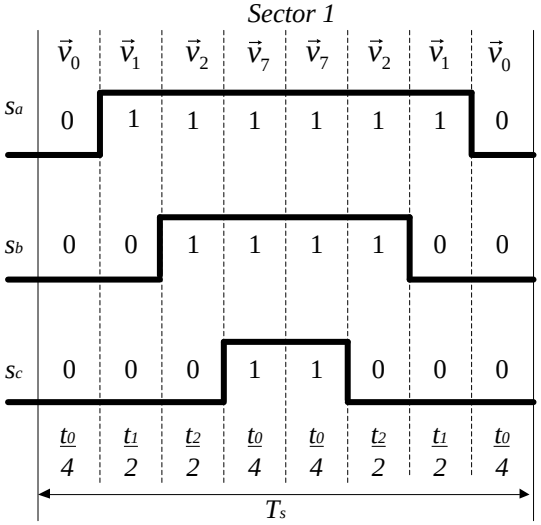

Figure. 6. 7-Segment Switching Sequence for V_{ref} in sector 1.

Finally, the basic operation of the proposed control method associated to a nonlinear load is summarize in Fig. 7. The switch control signals are derived from a Space Vector Modulator (SVM). Voltage references for the SVM are derived from the feedback linearization based DPC controllers. The references are computed by using the instantaneous PQ theory for currents and PQ-PLL for voltages. The compensation objective is to compensate harmonics in both voltage and current, reactive power compensation, and to regulate the DC bus during bidirectional active power exchange between the two active filters and the power system grid. Detailed description of different parts of UPQC is given hereafter.

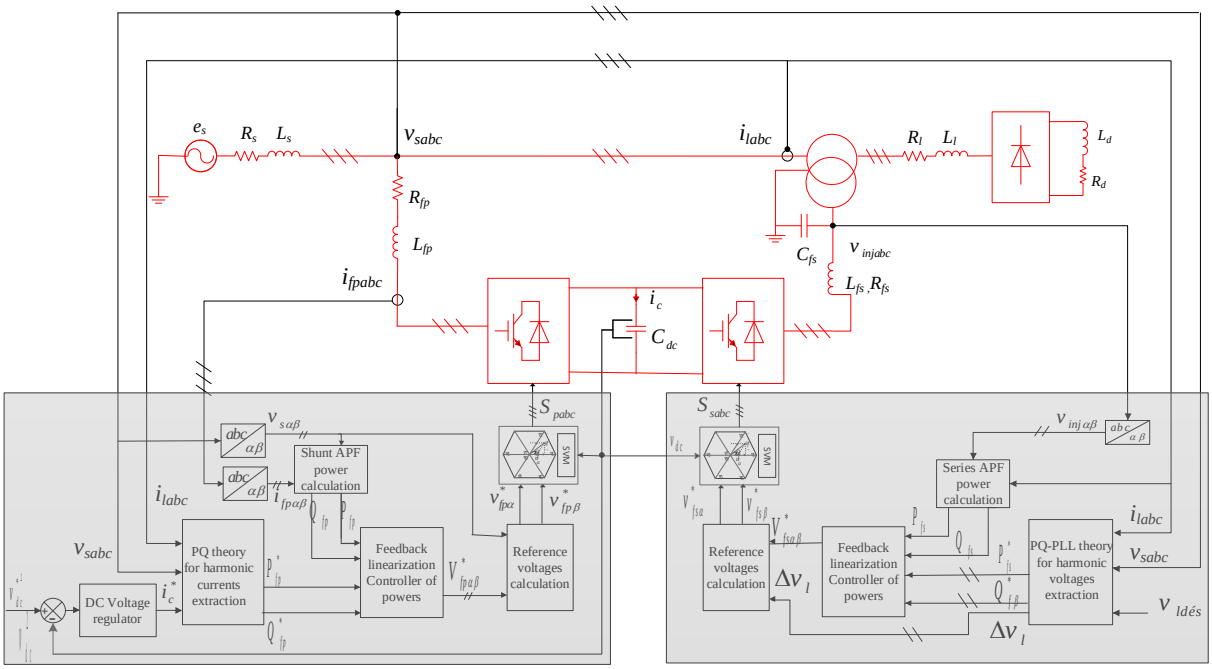

Figure. 7. Feedback linearization based DPC control scheme of the UPQC .

3. RESULTS AND DISCUSSION

Harmonic current and voltage filtering, reactive power compensation and performance of the UPQC with the proposed control have been examined in Matlab/Simulink environment, under nonlinear load variation and voltage sag. The parameters used in the present study are shown in Table I, while parameters and detailed study of linear control of the UPQC with PI controller is detailed in [25].

TABLE I
SYSTEM PARAMETERS

Parameter	value
RMS value of the source voltage	220 V
DC-link capacitor C_{dc}	8 mF
Source impedance Rs, Ls	3mΩ, 2.6 µH
Shunt filter impedance R_{fp}, L_{fp}	20 mΩ, 2.5 mH
Series filter impedance R_{fs}, L_{fs},C_{fs}	1.5 Ω, 3 mH, 0.1 mF
Line impedance R_l, L_l	10 mΩ, 0.3 µH
Diode rectifier load R_d , L_d	15 Ω, 2 mH
DC-link voltage reference	900 V
Switching frequency f_s	12 kHz
k_{p1}= k_{p2}	2100
k_{s1}= k_{s2}	1300
k_{dc}	250

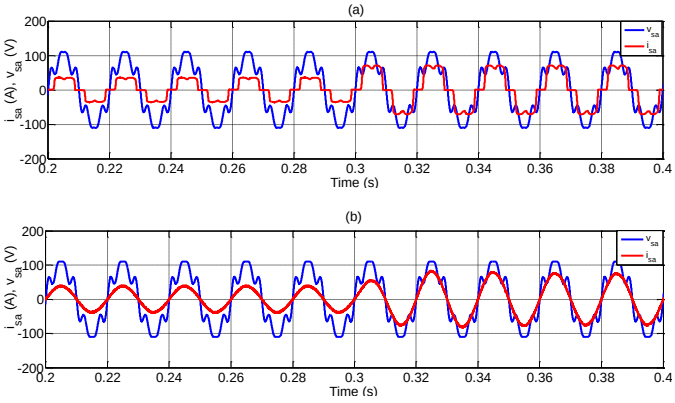

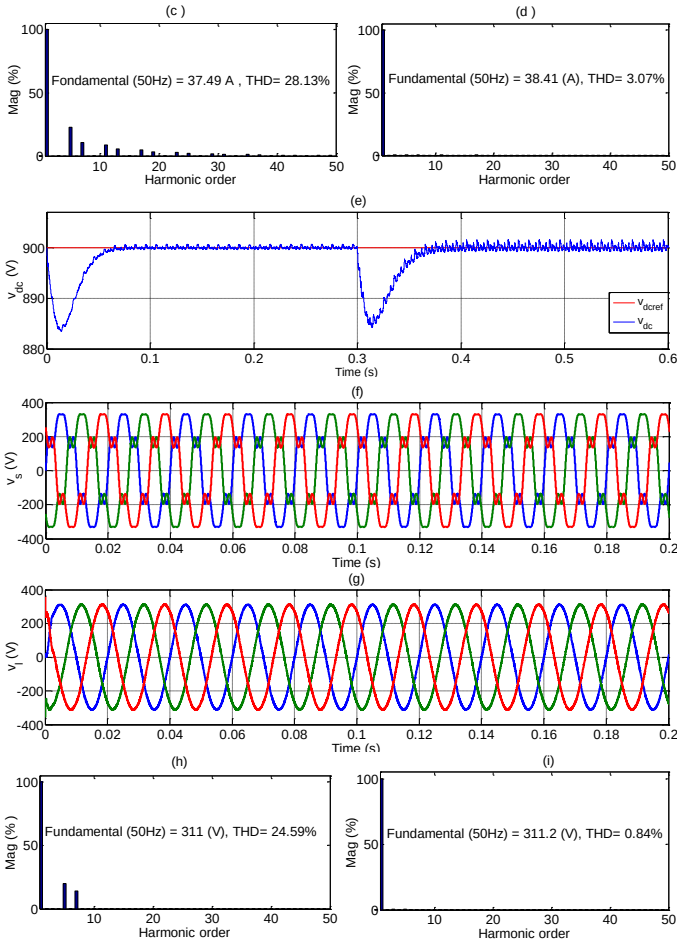

Fig. 7. Simulation results of the proposed controller. a): Source voltage and source current of a-phase before compensation, b): Source voltage and source current of a-phase after compensation, c): Harmonic spectrum of source current before compensation, d): Harmonic spectrum of source current after

compensation. e): DC-link voltage v_{dc}, f): Load voltage before compensation. g): Load voltage after compensation. h): Harmonic spectrum of load voltage before compensation, i): Harmonic spectrum of load voltage after compensation.

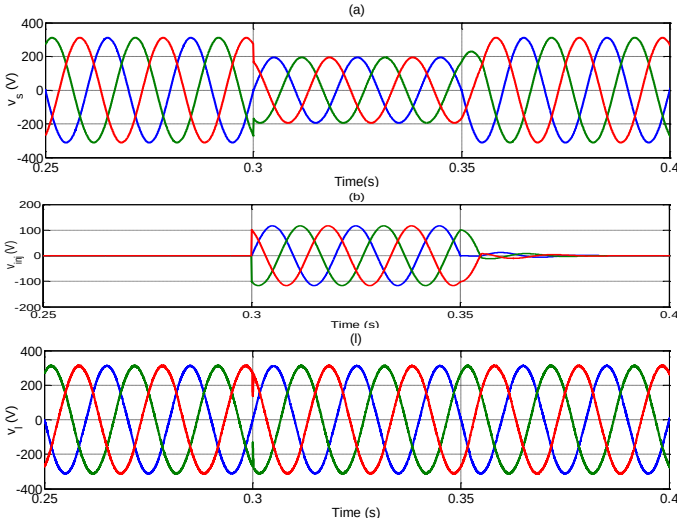

Fig. 8. Simulation results of the proposed sliding mode controller during a sag test. a): Source voltage during a sag. b): Injected voltage for compensating a sag. c): Load voltage during a sag after compensation.

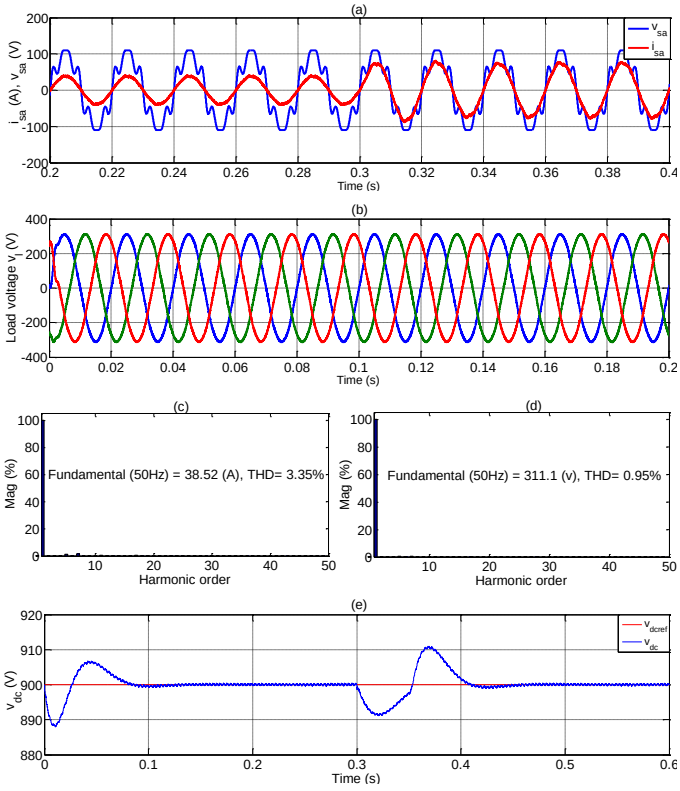

Fig. 9. Simulation results with PI controller. a): Source voltage and source current of a-phase before compensation, b): Load voltage after compensation. c): Harmonic spectrum of source current after compensation, d): Harmonic spectrum of load voltage after compensation. e): DC-link voltage v_{dc}.

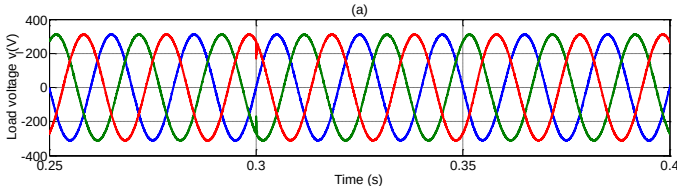

Fig. 10. Simulation results with PI controller during a sag test. a): Load voltage during a sag after compensation.

The dynamic behavior under a step change of the load at t = 0.3s is presented in Figs. 7.a and 7.b. It can be observed that the grid current become sinusoidal after the control application, and unity power factor operation is successfully achieved, even in this transient state.

In case of nonlinear control, the harmonic spectrums of AC grid current and load voltage before and after compensation are illustrated in Fig. 7.(c) and (d), for current, in Fig. 7.(h) and (i) for voltage. For linear control, the same spectrums are shown in Fig. 9.(c) and (d). It results that the UPQC decreases the total harmonic distortion (THD) in the grid currents from 28.13% to 3.35% with PI controller. However, with feedback linearization based DPC controller, the current THD is decreased down to 3.07%. Load voltage THD decreases from 24.59% to 0.95% with PI, while it is further decreases to 0.84% when feedback linearization based DPC controller is applied, which proves the effectiveness of the proposed nonlinear controller.

The UPQC was tested with sag in grid voltage, and the load voltage was again found very close to a sinusoidal voltage. So, the UPQC is able to produce the required compensating voltage components to keep constant load voltage.

The absence of an overshoot in DC voltage response during load change, low rise time and low THD, demonstrates the superiority of the feedback linearization based DPC controller compared to its counterpart traditional PI controller as illustrated in Table. II.

TABLE II
COMPARISON OF PI CONTROLLER WITH SLIDING MODE CONTROLLER

Factor	PI controller	FL-DPC controller
THDi (%)	3.35	3.07
THDv (%)	0.95	0.84
Charging of DC link (s)	0.11	0.08
Overshoot	+	-

4. CONCLUSION

In this paper a control design of the UPQC is carried out including its mathematical model, harmonic extraction methods for both currents and voltages. feedback linearization based DPC controller is derived to suppress currents and voltages harmonics. For the close power switches control, SVM approach has been used due to its benefits in term of fixed frequency of implementation. Simulation results show that in all the stages of system operation, the load side voltages and source side currents are very close to a sinusoidal shape. These results show clearly that UPQC controlled by feedback linearization based DPC offers much better performance compared to traditional controllers case.

REFERENCES

[1] Y. Lu, G. Xiao, X. Wang, F. Blaabjerg and D. Lu, “Control Strategy for Single-Phase Transformerless Three-Leg Unified Power Quality Conditioner Based on Space Vector Modulation”, IEEE Transactions on Power Electronics, vol. 31, no. 4, April 2016, pp. 2840-2849.

[2] R. M. Abdalaal and C. N. M. Ho, "Analysis and Validations of Modularized Distributed TL-UPQC Systems With Supervisory Remote Management System," in IEEE Transactions on Smart Grid, vol. 12, no. 3, pp. 2638-2651, May 2021, doi: 10.1109/TSG.2020.3044992.

[3] Jayanti Sarker, S.K. Goswami, “Optimal Location of Unified Power Quality Conditioner in Distribution System for Power Quality Improvement”, International Journal of Electrical Power & Energy Systems, Vol. 83, December 2016, pp. 309-324.

[4] N. Patnaik, A. K. Panda, “Performance analysis of a 3 phase 4 wire UPQC system based on PAC based SRF controller with real time digital simulation”, International Journal of Electrical Power & Energy Systems, Volume 74. January 2016, pp. 212-221.

[5] M. Anand and P. Kumar, "Fuzzy Controller based Topologies of NS-UPQC and B4-UPQC," 2020 IEEE International Conference on Advent Trends in Multidisciplinary Research and Innovation (ICATMRI), 2020, pp. 1-7, doi: 10.1109/ICATMRI51801.2020.9398396.

[6] Peng Li, Yuwei Li, Ziheng Yin, "Realization of UPQC H∞ coordinated control in Microgrid", International Journal of Electrical Power & Energy Systems, Vol. 65, February 2015, pp. 443-452.

[7] S. R. Arya, S. J. Alam and P. Ray, "Control algorithm based on limit cycle oscillator-FLL for UPQC-S with optimized PI gains," in CSEE Journal of Power and Energy Systems, vol. 6, no. 3, pp. 649-661, Sept. 2020, doi: 10.17775/CSEEJPES.2019.01030.

[8] DAHDOUH, ADEL, Barkat, Said, Aissa, Chouder,"A Combined Sliding Mode Space vector Modulation Control of the Shunt Active Power Filter Using Robust Harmonic Extraction Method A Combined Sliding Mode Space vector Modulation Control of the Shunt Active Power Filter Using Robust Harmonic Extraction Method". Algerian Journal of Signals and Systems. Vol. 1, 2016, pp. 37-46. 10.51485/ajss.v1i1.17.

[9] M. Bouzidi, A. Benaissa, S. Barkat, "Application of feedback linearization to the virtual flux direct power control of three-level three-phase shunt active power filter", International review of electrical engineering, Vol. 5, No. 3, pp.1128-1140, 2012..

[10] T. Koroglu, A. Tan, M. M. Savrun, M. U. Cuma, K. C. Bayindir and M. Tumay, "Implementation of a Novel Hybrid UPQC Topology Endowed With an Isolated Bidirectional DC–DC Converter at DC link," in IEEE Journal of Emerging and Selected Topics in Power Electronics, vol. 8, no. 3, pp. 2733-2746, Sept. 2020, doi: 10.1109/JESTPE.2019.2898369.

[11] R. H. Yang and J. X. Jin, "Unified Power Quality Conditioner With Advanced Dual Control for Performance Improvement of DFIG-Based Wind Farm," in IEEE Transactions on Sustainable Energy, vol. 12, no. 1, pp. 116-126, Jan. 2021, doi: 10.1109/TSTE.2020.2985161.

[12] S. Devassy and B. Singh, "Performance Analysis of Solar PV Array and Battery Integrated Unified Power Quality Conditioner for Microgrid Systems," in IEEE Transactions on Industrial Electronics, vol. 68, no. 5, pp. 4027-4035, May 2021, doi: 10.1109/TIE.2020.2984439.

[13] M. A. Mansor, K. Hasan, M. M. Othman, S. Z. B. M. Noor and I. Musirin, "Construction and Performance Investigation of Three-Phase Solar PV and Battery Energy Storage System Integrated UPQC," in IEEE Access, vol. 8, pp. 103511-103538, 2020, doi: 10.1109/ACCESS.2020.2997056.

[14] J. Yu, Y. Xu, Y. Li and Q. Liu, "An Inductive Hybrid UPQC for Power Quality Management in Premium-Power-Supply-Required Applications," in IEEE Access, vol. 8, pp. 113342-113354, 2020, doi: 10.1109/ACCESS.2020.2999355.

[15] Y. Harbouche, L. Khellache and R. Abdessemed, "UVTG Control Strategy for Three Phase Four Wire UPQC to Improve Power Quality", International Electrical Engineering Journal, vol. 6, No. 9, 2015, pp. 1988-1993.

[16] S. A. O. da Silva, L. B. G. Campanhol, G. M. Pelz and V. de Souza, "Comparative Performance Analysis Involving a Three-Phase UPQC Operating With Conventional and Dual/Inverted Power-Line Conditioning Strategies," in IEEE Transactions on Power Electronics, vol. 35, no. 11, pp. 11652-11665, Nov. 2020, doi: 10.1109/TPEL.2020.2985322..

[17] S. J. Alam and S. R. Arya, "Control of UPQC based on steady state linear Kalman filter for compensation of power quality problems," in Chinese Journal of Electrical Engineering, vol. 6, no. 2, pp. 52-65, June 2020, doi: 10.23919/CJEE.2020.000011.

[18] A. Ozdemir.and Z. Ozdemir., "Digital current control of a three-phase four-leg voltage source inverter by using p-q-r theory" Power Electronics, IET , Vol.7, No.3, March 2014, pp.527-539.

[19] L.S Czarnecki, "Constraints of instantaneous reactive power p-q theory" in Power Electronics, IET , vol.7, no.9, September 2014, pp.2201-2208.

[20] S. K. Dash and P. K. Ray, "A New PV-Open-UPQC Configuration for Voltage Sensitive Loads Utilizing Novel Adaptive Controllers," in IEEE Transactions on Industrial Informatics, vol. 17, no. 1, pp. 421-429, Jan. 2021, doi: 10.1109/TII.2020.2986308.

[21] R. Guzman, L.G Vicuna,J. Morales, M. Castilla, J. Matas,. "Sliding-Mode Control for a Three-Phase Unity Power Factor Rectifier Operating at Fixed Switching Frequency" in Power Electronics, IEEE Transactions on , vol.31, no.1, Jan. 2016, pp.758-769.

[22] A. Chebabhi, M.K Fellah and M.F Benkhoris "Sliding Mode Controller for Four Leg Shunt Active Power Filter to Eliminating Zero Sequence Current, Compensating Harmonics and Reactive Power with Fixed Switching Frequency ", Serbian Journal Of Electrical Engineering, Vol. 12, No. 02, june 2015, pp. 205- 218.

[23] K.Ramya and R.Prakash "Comparative Analysis of PWM Techniques for Three Level Diode Clamped Voltage Source Inverter", International Journal of Power Electronics and Drive System, Vol. 5, No. 01, July-2014, pp. 15- 23.

[24] J. Han, X. Li, Y. Jiang and S. Gong, "Three-Phase UPQC Topology Based on Quadruple-Active-Bridge," in IEEE Access, vol. 9, pp. 4049-4058, 2021, doi: 10.1109/ACCESS.2020.3047961.

[25] DAHDOUH, ADEL, Barkat, Said, Aissa, Chouder," SLIDING MODE BASED ON SPACE VECTOR MODULATION CONTROL OF THE UNIFIED POWER QUALITY CONDITIONER". Mediterranean Journal of Measurement and Control. Vol. 13, 2017, pp. 686-694.

BIOGRAPHIES

Adel Dahdouh received his License and Master degrees in Electrical Engineering from Mohamed Boudiaf University of M'sila, Algeria, in 2013 and 2015 respectively. Currently, he is a researcher in Applied Automation and Industrial Diagnostic of Djelfa (LAADI). His research interest includes control of power converters, power quality enhancement, micro-grids and energy management systems.

Lakhdar MAZOUZ, is an assistant lecturer and researcher at the department of Electrical Engineering, University of Djelfa Algeria. He received the licence degree on electrical engineering from the University of Laghouat, Algeria. He received PhD degree in 2017 from the Djillali Liabes University of Sidi Bel-Abbes (Algeria) and the Magister degree, from the same University in 2010. He is current research interests are: the VSC-HVDC link, the FACTS and the Offshore Wind Farms.

Brahim Elkhalil Youcefa received his License and Master degrees in Electrical Engineering from Mohamed Boudiaf University of M'sila, Algeria, in 2013 and 2015 respectively. He received PhD degree in 2020 from the Djillali Liabes University of Sidi Bel-Abbes (Algeria) His research interest includes control of power converters, power quality and modeling and control of renewable energy sources